The development of chemical tools to study the interplay of ubiquitination and ADPribosylation

Kloet, M.S.

Chapter 3

A photo-activatable histidine reactive probe to capture Legionella effectors

Max S. Kloet[a], Gerbrand J. van der Heden van Noort[a]*

a Department of Cell and Chemical Biology, Leiden University Medical Centre, Leiden, The Netherlands

Published in the Frontiers in Molecular Biosciences (2024) – 11

Introduction

Although histidine residues occur infrequently in nature (<2.5%), they often play a critical role as key residues in over 15% of enzyme active sites.[1] Specifically, histidines are present in for instance the active sites of the ubiquitin-specific protease (USP) and histone deacetylases enzyme families as well as in the Legionella effector enzymes SdeA and DupA.[2–4]

To effectively design a probe that specifically targets catalytic histidine residues, it is crucial to incorporate an appropriate reactive moiety or warhead tailored to the reactivity of histidine. The challenging aspect of targeting histidine lies in its moderate nucleophilicity compared to other residues like cysteine or lysine, making selective targeting a difficult task, exemplified by early attempts using simple molecules like iodomethane.[5,6] More recently, a study utilizing a library of electrophilic warheads on ubiquitin, containing a single histidine (His68), found diethyl vinylphosphonate and 2-cyclohexenone although moderately reactive to be chemoselective towards histidine.[7] In the same study vinyl sulfonates were also investigated for their histidine reactivity, proving to be reactive yet also showing cross-reactivity to lysine residues. Despite this, and the encountered reactivity to cysteine by us (chapter 2) and others[8], vinyl sulfonates were effectively used to covalently immobilize proteins by reacting to a non-native histidine-tag.[9] Another interesting warhead explored for histidine targeting is the thiophosphorodichloridate[10], effectively labeling histidine on isolated proteins and in cell lysates.[10] Analysis of the labeled proteins using mass spectrometry primarily showed targeting of solvent-exposed histidine's rather than active site histidine's. Notably, the dichloridate reagent itself, demonstrated instability under aqueous conditions, limiting its applicability.

However, next to finding a suitable warhead, specific targeting of active site histidine residues can be challenging due to their embedding within the protein's structure, often requiring ligand-directed approaches for enzyme targeting.[11] In 2009, ligand-directed tosyl targeting utilizing an endogenous ligand and a cleavable tosylate as a warhead was successful in labeling histidine amongst other residues *in vivo*.[11,12] The first targeting of an active site histidine was demonstrated on methionine aminopeptidase-2. By synthesizing its natural substrate fumagillin, and introducing an epoxide warhead at the site where the histidine in the catalytic triad is located (demonstrated by docking), a covalent bond between the histidine and the warhead could be formed.[13] Other examples of active site targeting include the covalent targeting of the reactive histidine in the vitamin D receptor using a ligand possessing an enone α,β-unsaturated system,[14] a warhead also effective in targeting His247 of the catalytic triad in the receptor DWARF14.[15] Additionally, fluorosulfonylbenzoyl has been

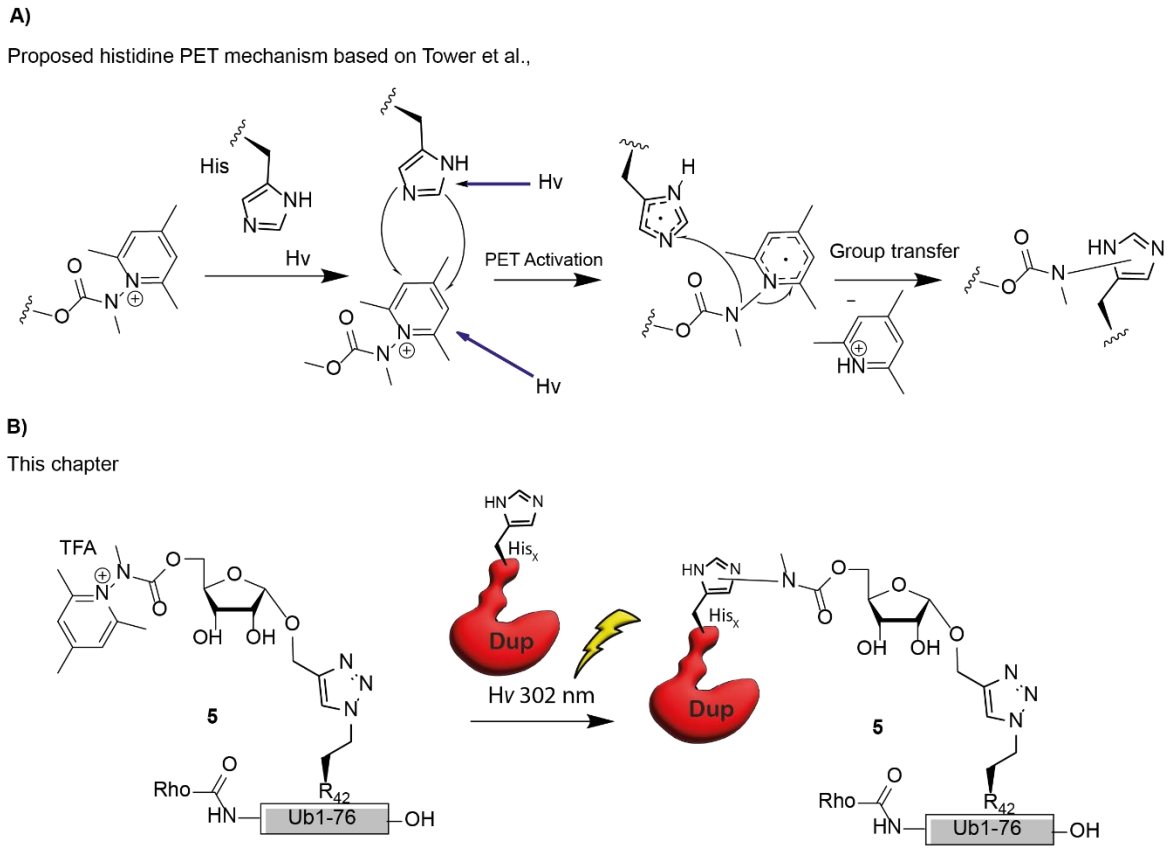

Fig. 1. Pyridinium reagents photo-reacting to histidine. **A**) A proposed mechanism covalently binding histidine based on the tryptophan mechanism by Tower *et al*. **B**) The proposed covalent labeling of an active site His in DupA via a PET photoreaction to Ub pyridinium phosphoribose probe **5**, the aim of this chapter.

shown to induce loss of activity for the bovine mitochondrial FI-ATPase after reacting with His-427.[16]

Based on our experience with vinyl sulfonate probes targeting Cys196 of DupA/B in chapter 2, we set out to induce a His-selective reaction in the active site of DupA using a similar ligand-directed approach. To achieve this and circumvent side reactions to nucleophilic amino acid side chains, we used the photoactivation capability of His and changed the warhead. Katritzky-type[17] pyridinium salts[18,19] are recognized for their participation in photo-crosslinking reactions through a proposed photoinduced electron transfer (PET) mechanism selectively targeting His (**Fig. 1A**) and Trp.[18,20] Given that Trp is not present in the active site of DupA and previous findings suggest the pyridinium moiety does not react with Cys, a pyridinium warhead equipped probe seems a feasible approach to circumvent Cys196 and react to one of the active site His residues in DupA (**Fig. 1B**).

Results & Discussion

Chemical synthesis of photoactivatable Ub pyridinium probe (5)

Hacker and co-workers observed significant labeling of histidine residues in the proteome when using an Katritzky-type pyridinium warhead [17] upon performing photo-cross-coupling in bacterial lysate.[20] The here presented approach entails a ligand directed approach of a phosphoribose-Ub substrate mimic equipped with a pyridinium His-reactive warhead to the active site of Legionella effectors based on their affinity for (phosphoribosyl)ubiquitin intended to induce a covalent-bond forming reaction with one of the two active site His residues (His67 and His189) upon photo-activation.

In order to incorporate the photoactivable warhead in the probe, synthesis was initiated from ribose **1,** which is equipped with an anomeric propargyl and isopropylidene protection, and previously reported in chapter 2.[18,21,22] Activation of the primary alcohol in **1** by 1,1-carbonyldiimidazole (CDI) and subsequent substitution by methyl hydrazine afforded the crude methyl hydrazide[18,21] **2**. Treating this compound with 2,4,6-trimethylpyrylium tetrafluoroborate in ethanol effectively formed the pyridinium riboside **3**, which was used as crude in the next step.[18,21,22] The subsequent deprotection of the isopropylidene proceeded uneventfully and isolation by preparative-HPLC yielded **4** in 16% over three steps. To finalize the probe synthesis, deprotected riboside **4** was conjugated to Rho-Ub (Arg42 → azido homoalanine) (reported in chapter 2) through CuAAC affording the pyridinium riboside ubiquitin probe **5**. The probe bears a rhodamine to visualize the DupA-probe **5** complex formation by in-gel fluorescence.

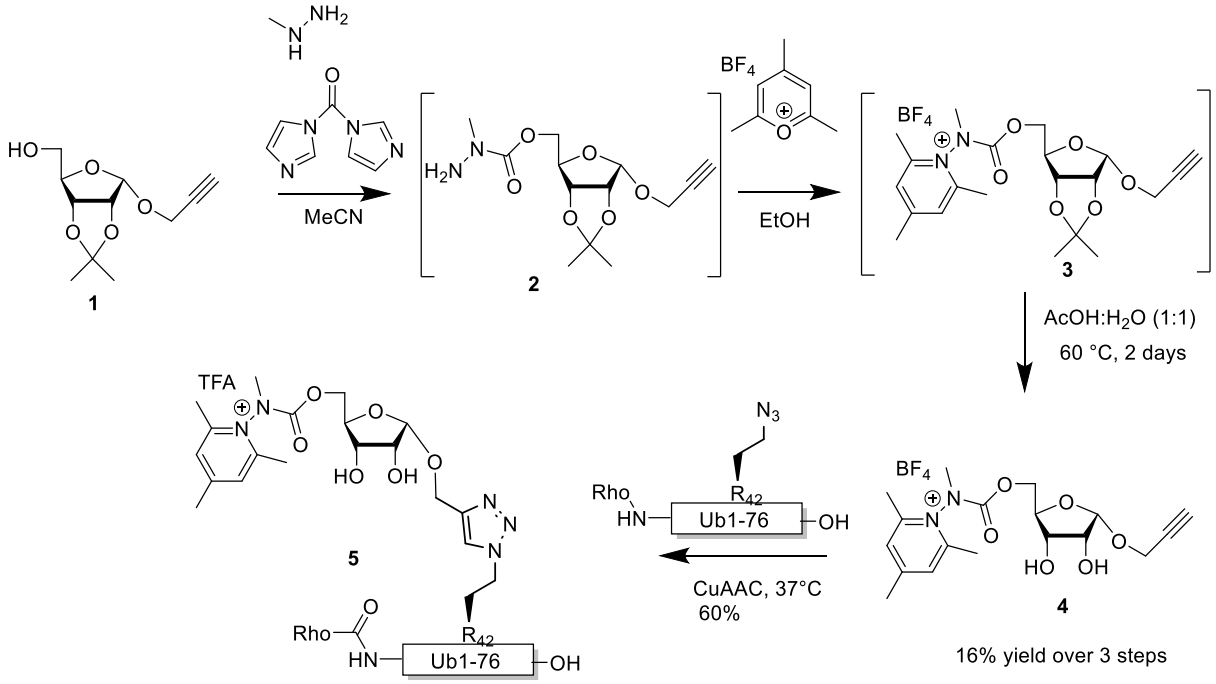

Scheme 1. Synthesis of Ub-pyridinium probe **5**.

Probe photoactivation and probe 5-DupA cross-coupling analyzed by mass spectrometry

To assess photo-activation of probe **5** we irradiated the probe (302 nm) for 1 hour and activation of the *N*-*N* bond was observed using high-resolution mass-spectrometry, as indicated by loss of the pyridinium moiety (HR-MS: deconvoluted mass = 9.117 Da, Δ = -120 Da) and concomitant loss of the carbamate moiety (HR-MS: deconvoluted mass = 9.060, Δ = -177), **Supplementary Fig. 1A**). However, noise is observed in the <6.000 Da range, potentially attributed to ROS-induced oxidation and photodegradation of ubiquitin, as similarly observed by Tower *et al*., using the pyridinium warhead in a Katritzky-type PET cross-coupling.[18] Increased product formation has been reported when adding glutathione (GSH) to the PET cross-coupling as reactive oxygen species (ROS) scavenger.[18,23] Indeed, the addition of GSH (1 mM) resulted in cleaner activation of the probe, indicating a protective role of the additive. However, a covalent adduct between **5** and GSH was observed as side reaction (HR-MS: deconvoluted mass = 9.423 Da / 9.380 Da, **Supplementary Fig. 1B**), a reaction also reported earlier.[18,24] We lowered the GSH concentration to 300 µM and followed activation of the probe after 1, 15, 30 and 60 minutes (**Supplementary Fig. 2**). Whereas significant amounts of unactivated probe remain up to 30 minutes irradiation, after 60 minutes almost all probe has been activated.

After showing activation of the probe to be effective, the next objective was to photo-cross-link Ub probe **5** to recombinant DupA. First, DupA was incubated with probe **5** (10 eq.) and irradiated for 1 hour in absence of GSH and moderate complex formation could be detected using mass-spectrometry (**Supplementary Fig. 3A**. HR-MS: deconvoluted mass = 48.561 Da). In the absence of reductive agents multiple presumably oxidized states of the complex but also DupA alone could be observed, complicating analysis. Subsequently, when including GSH (1 mM) as additive in the photo-induced reaction of probe **5** and DupA significantly less conjugate formation and substantial formation of a DupA-GSH adduct (HR-MS: deconvoluted mass = 39.763, Δ = +320) were detected (**Supplementary Fig. 3B)**. Although mass spectrometric analysis of the crosslinking reaction is not ideal, we could conclude that photoactivation of the probe is feasible and the formation of the DupA-probe **5** conjugate could be effected. Additionally, GSH as additive has a favorable protective ROS scavenging role, yet also seems to impede the cross-coupling efficiency of Ub probe **5** to DupA.

SDS-PAGE analysis of probe 5-DupA and -SdeA$_{PDE}$ photo-cross-linked conjugates

To more efficiently visualize complex formation, a gel-based analysis of the reaction between probe **5** and target protein DupA was conducted (**Fig. 2A**). We screened the above used concentrations of GSH as well as the non thiol reductant TCEP to investigate the impact on conjugate formation and ROS-protection. Without additive, decent crosslinking was observed, as visualized by Coomassie staining and a rhodamine fluorescence scan. In contrast, irradiating the Rho-Ub (Arg42 to azido homoalanine) mutant that does not contain the photo-activatable group did not result in formation of the crosslinked Ub-DupA complex (**Supplementary Fig. 4)**. Consistent with the MS results, 1 mM of GSH proved not to be beneficial for product formation, however seemed to be protective to enzyme integrity as reflected by a reduction of high

molecular weight smears. Lowering the GSH concentration (300 µM) improved product formation, albeit with a slight increase in the formation of high molecular weight aggregates compared to the 1 mM GSH conditions. These aggregates are also present when DupA itself is irradiated and hence are not caused by the probe. Addition of tris(2-carboxyethyl)phosphine (TCEP), a reducing agent not acting as a ROS scavenger did not prevent smear formation and hence is no suitable alternative in this reaction. Overall, decreasing the GSH concentration from 1 mM to 300 µM increased the conversion of the photo-cross-coupling while suppressing side product formation. We subsequently followed complex formation over time and although 60 minutes irradiation leads to a larger conversion into the probe-DupA complex also significant photo-degradation can be seen. Hence the 15 minute irradiation time-point was selected as compromise between optimal crosslinking efficiency and preserving protein integrity (**Fig. 2B**).

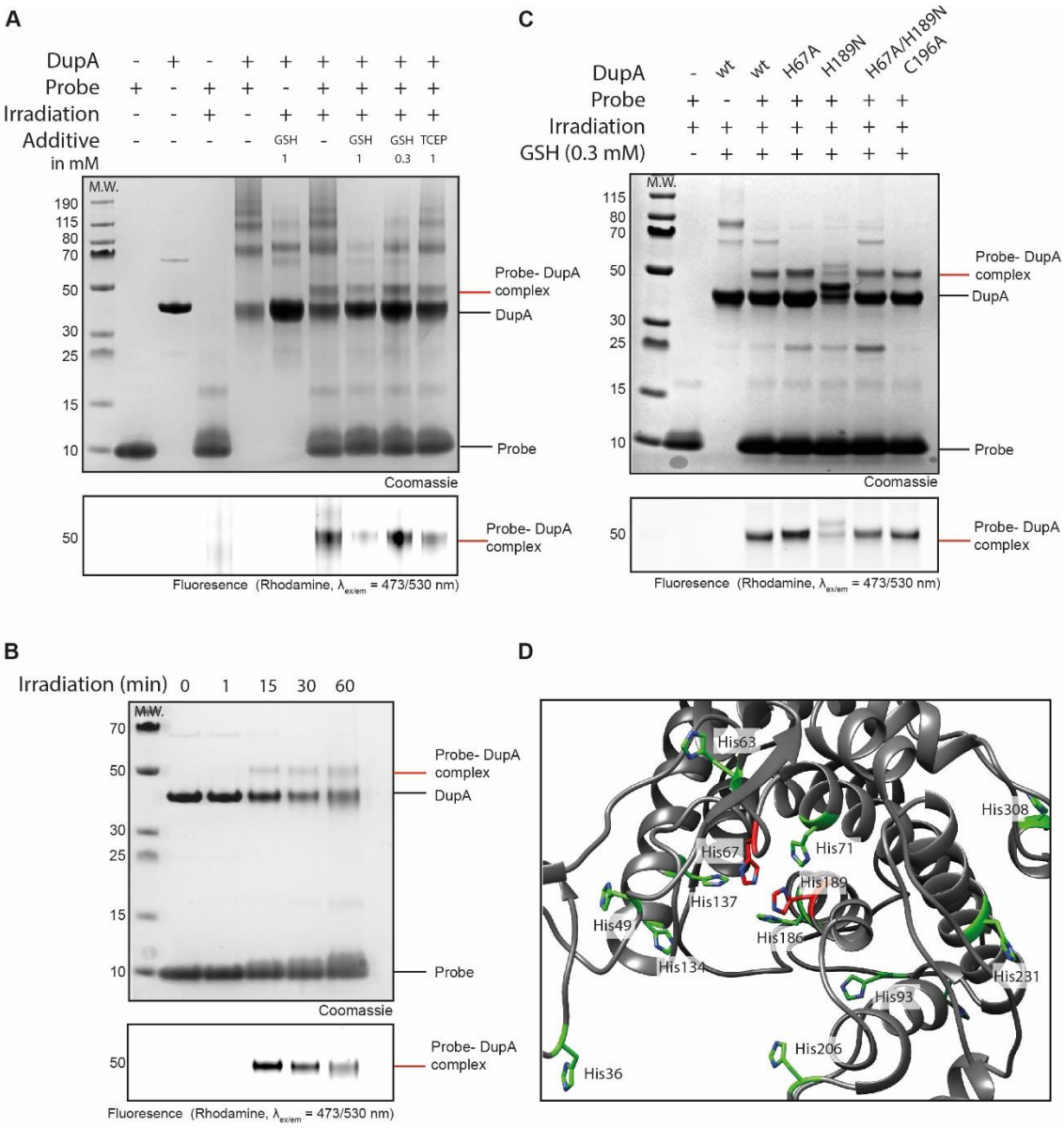

Fig 2. Ub-pyridinium probe **5** crosslinks to DupA upon photo-activation. **A**) SDS-PAGE gel showing complex formation between probes **5** and DupA wt. 10 equivalents of probe was used and GSH and TCEP were screened as additives. Irradiation for 60 min. Upper panel: Coomassie stained, bottom panel: Rhodamine fluorescence scan ($\lambda_{ex/em}$ = 473/530 nm). **B**) SDS-PAGE gel showing complex formation between probes **5** and DupA wt. 10 equivalents of probe in the presence of GSH (300 µM) and irradiation for indicated times. **C**) Mutagenesis on DupA and reactivity of the mutants to probe **5** in the presence of GSH (300 µM) as additive and irradiation for 15 minutes. **D**) Crystal structure of DupA wt (PDB: 6B7O) (grey) highlighting all histidine residues (green) and catalytic histidines (red).

To investigate whether probe **5** reacts with the active site triad His67 or His189, we monitored complex formation on DupA-(His67 to Ala), DupA–(His189 to Asn) and DupA-(His67 to Ala/ His189 to Asn) mutants. Photo-cross-linking of the probe to the DupA (His189 to Asn) mutant demonstrated a reduction in labelling compared to DupA wild type (wt) and all other mutants, as evidenced by SDS-PAGE Coomassie and a

fluorescence scan (**Fig. 2C**). This reduction indicates a disability of the probe to react with the His189 to Asn mutant, although some residual labeling is still visible for this mutant. The double mutant DupA (His67 to Ala/ His189 to Asn) however does not show a marked reduction in labelling efficiency. Interestingly, upon closer examination of the crystal structure (PDB: 6B7O), multiple additional histidine residues in the catalytic cleft were observed (**Fig. 2D**). The presence of other His residues might explain residual labeling in all samples, as upon mutagenesis of the active site residues the probe could still potentially bind one of the other His in the same pocket. Of note, the Cys196 to Ala mutant was labeled to comparable extent as DupA wt, suggesting the probe has no reactivity towards the Cys residue.

DupA and $SdeA_{PDE}$ are structurally homologous featuring a similar catalytic triad (**Fig. 3B,C**), and consequently we set out to verify if an active site His in the PDE domain of SdeA could also be targeted using probe **5**. Initially, only small traces of probe **5**-$SdeA_{PDE}$ conjugate formation were observed using 10 equivalents of probe. Gratifyingly, increasing the amount of probe to 100 equivalents improved the conversion and resulted in a clear visual band above the 70 kDa marker, the expected molecular weight region of the conjugate (**Fig. 3A**). Moreover, this band is clearly detectable in the fluorescence channel and not observed in the controls. The conversion is moderate compared to DupA wt and might be attributed to a different engagement of SdeA by Ub probe **5**.[25]

To provide an indication of selectivity of our probe to Legionella effector enzymes, the pyridinium probe was reacted with enzymes NRK-1, UCHL-3 and USP-21. When incubating **5** with NRK-1, which could potentially cross-react due to recognition of the riboside-moiety in the probe as a nucleoside-like substrate, no conjugate formation was observed after irradiation (**Supplementary Fig. 5**). Subsequently, probe **5** was irradiated in the presence of deubiquitinating proteases, UCHL3 or USP21. As these DUBs recognize ubiquitin as substrate and contain a histidine in their active site, they may react as off-targets. Interestingly, UCHL-3 exhibited some reactivity to the probe, whereas USP21 showed no reactivity (**Supplementary Fig. 5**). To verify the extent of off-target reactivity and validate crosslinking potential of probe **5** towards DupA in a more complex environment, we incubated the probe in HEK cell lysate containing spiked in DupA and performed photo-activation followed by SDS-PAGE analysis (**Supplementary Fig. 6**). The DupA-probe conjugate can be appreciated in the fluorescent channel running at the same apparent molecular weight as the complex formed in buffer, whereas either omission of spiking in DupA or irradiation does not lead to the complex being formed in the lysate.

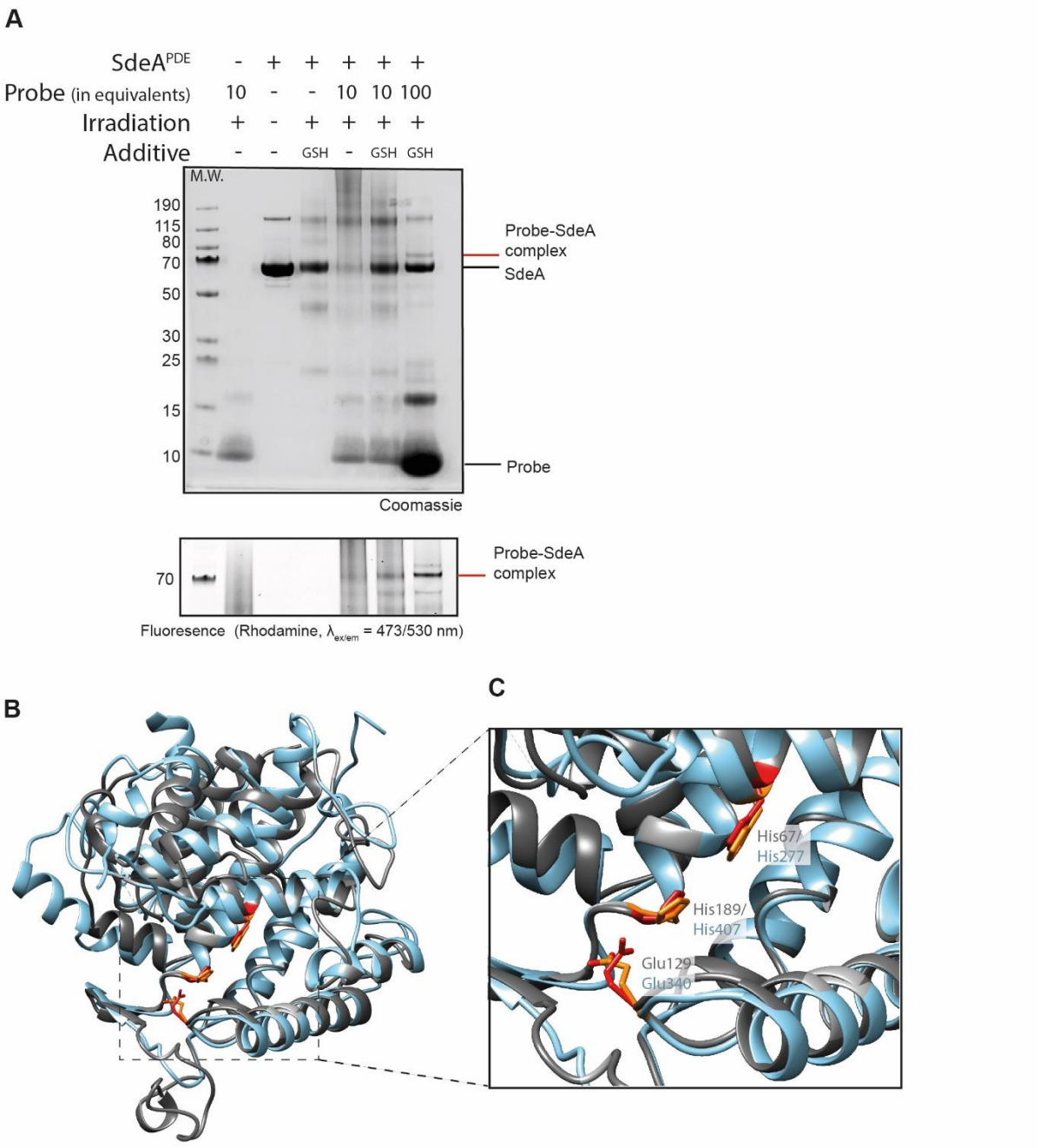

Fig. 3. Ub-pyridinium probe **5** binds SdeA PDE upon photo-activation. **A)** SDS-PAGE showing complex formation between probes **5** and SdeA PDE (10 eq. or 100 eq. of probe). Irradiation was performed for 1 hour at 302 nm. Upper panel: Coomassie stained, bottom panel, zoom in on Rhodamine fluorescence scan ($\lambda_{ex/em}$ = 473/530 nm). **B)** Superimposition of DupA (PDB:6B7O) (grey) and the PDE domain of SdeA (PDB:6G0C) (light blue), **C)** Zoom in on the catalytic triads of DupA and SdeA$_{PDE}$.

Conclusion

In this chapter, we show a methodology to incorporate a Katritzky-type pyridinium warhead in a Ub-based probe to induce a photo-cross-coupling that could potentially be used to selectively label His residues in the active site of Legionella effector enzymes involved in the unconventional phosphoribosyl ubiquitination pathway. Installing this warhead on the primary alcohol of an anomeric alkyne equipped riboside proved to be effective in 16% over 3 steps after HPLC-purification. Subsequently, conjugation through CuAAC of the formed pyridinium riboside **4** to a Rhodamine labelled Ub_{76} (Arg42 to azido homoalanine) mutant resulted in the Ub-phosphoribose mimicking probe **5**. Photoactivation of the probe was initially analyzed by HR-MS, showing near-complete activation of the probe after 1h of irradiation (302 nm). However, due to multiple oxidations and potential photo-degradation occurring during the reaction, analysis of the complex formation between probe **5** and DupA wt proved to be difficult using mass spectrometry. Gratifyingly, in-gel fluorescence and Coomassie staining on SDS-PAGE effectively visualized the formation of the probe-DupA conjugate after irradiation. To our knowledge this is the first example of the pyridinium based photochemical reaction to cross-couple two proteins. Optimization of the reaction conditions involved the application of GSH as additive, indicating a protective role of GSH, consistent with findings by Tower *et al*.[18] In order to pinpoint which amino acid in DupA reacts with probe **5**, the photoreaction was performed on DupA active site mutants (His67 to Ala), (His189 to Asn) and (His67 to Ala/His189 to Asn). Strikingly, compared to the DupA wt, reduced conversion is observed for the His189 to Asn mutant, whereas all other mutants including the Cys196 to Ala mutant retained the same level of reactivity towards the probe. Taken together, this initial data is inconclusive to determine the binding site of probe **5**. Although reactivity of the probe towards the single His189 mutant is reduced, the double His67/His189 mutant labels comparably to wildtype DupA. Due to the presence of other His residues not taken along in this mutational studies, it cannot be excluded that upon mutating one specific His residue the probe is redirected towards another His residue. The cross-coupling of the probe to $SdeA_{PDE}$ proved to be effective as well, although the observed conversion is modest or requires a larger excess of probe. Although both SidE and Dup Legionella effectors thus react with probe **5**, the probe also labelled recombinant UCHL-3, suggesting potential off-target reactivity. Performing crosslinking in HEK cell lysate by adding DupA and probe highlights the translatability of this procedure to more complex biological systems. In conclusion the probe demonstrated effective photo-cross-coupling to the Legionella effectors DupA and $SdeA_{PDE}$ and holds promise to monitor Legionella effector enzymes involved in PR-ubiquitination in Legionella infected cells.

References

1. Bartlett, G. J., Porter, C. T., Borkakoti, N. & Thornton, J. M. Analysis of catalytic residues in enzyme active sites. *J Mol Biol* **324**, 105–121 (2002).

2. Haberland, M., Montgomery, R. L. & Olson, E. N. The many roles of histone deacetylases in development and physiology: Implications for disease and therapy. *Nature Reviews Genetics* **10**, 32–42 (2009).

3. Komander, D., Clague, M. J. & Urbé, S. Breaking the chains: Structure and function of the deubiquitinases. *Nature Reviews Molecular Cell Biology* **10**, 550–563 (2009).

4. Kalayil, S. *et al.* Insights into catalysis and function of phosphoribosyl-linked serine ubiquitination. *Nature* **557**, 734–738 (2018).

5. Takahashi', K. The Structure and Function of Ribonuclease T1XXI. Modification of Histidine Residues in Ribonuclease Tl with Iodoacetamide. *J. Biochem* **80**, (1976).

6. Roberts, M. F., Deems, R. A., Mincey, T. C. & Dennis, E. A. Chemical Modification of the Histidine Residue in Phospholipase A, (Naja Naja Naja). *The journal of biological chemistry* **252**, 2405-2411 (1911).

7. Joshi, P. N. & Rai, V. Single-site labeling of histidine in proteins, on-demand reversibility, and traceless metal-free protein purification. *Chemical Communications* **55**, 1100–1103 (2019).

8. Dalton, S. E. & Campos, S. Covalent Small Molecules as Enabling Platforms for Drug Discovery. *ChemBioChem* **21**, 1080–1100 (2020).

9. Li, M. *et al.* Site-Specific and Covalent Immobilization of His-Tagged Proteins via Surface Vinyl Sulfone-Imidazole Coupling. *Langmuir* **35**, 16466–16475 (2019).

10. Jia, S., He, D. & Chang, C. J. Bioinspired thiophosphorodichloridate reagents for chemoselective histidine bioconjugation. *J Am Chem Soc* **141**, 7294–7301 (2019).

11. Tamura, T. & Hamachi, I. Chemistry for Covalent Modification of Endogenous/Native Proteins: From Test Tubes to Complex Biological Systems. *J Am Chem Soc* **141**, 2782–2799 (2019).

12. Tsukiji, S., Miyagawa, M., Takaoka, Y., Tamura, T. & Hamachi, I. Ligand-directed tosyl chemistry for protein labeling in vivo. *Nat Chem Biol* **5**, 341–343 (2009).

13. Liu, S., Widom, J., Kemp, C.W., Crews, C.M., Clary, J. Structure of Human Methionine Aminopeptidase-2 Complexed with Fumagillin. *Science (1979)* **282**, 1324–1327 (1998).

14. Yoshizawa, M. *et al.* Identification of the Histidine Residue in Vitamin D Receptor That Covalently Binds to Electrophilic Ligands. *J Med Chem* **61**, 6339–6349 (2018).

15. De Saint Germain, A. *et al.* An histidine covalent receptor and butenolide complex mediates strigolactone perception. *Nat Chem Biol* **12**, 787–794 (2016).

16. Zhuo, S., Garrod, S., Miller, P. & Allison, W. S Irradiation of the Bovine Mitochondrial F1-ATPase Previously Inactivated with 5'-p-Fluorosulfonylbenzoy1-8-azido-[3H]adenosine Cross-links His-427 to Tyr-345 within the Same beta Subunit*. The Journal of biological chemistry **267,** 12916-12927 (1992).

17. Bapat, R. B. J. *et al.* Pyridines as leaving groups in synthetic transformation: Nucleophilic displacements of amino groups, and novel preparations of nitriles and isocyanates. *Tetrahedron Letters* **31***,* 2691-2694 (1976).

18. Tower, S. J., Hetcher, W. J., Myers, T. E., Kuehl, N. J. & Taylor, M. T. Selective Modification of Tryptophan Residues in Peptides and Proteins Using a Biomimetic Electron Transfer Process. *J Am Chem Soc* **142**, 9112–9118 (2020).

19. Hoopes, C. R. *et al.* Donor-Acceptor Pyridinium Salts for Photo-Induced Electron-Transfer-Driven Modification of Tryptophan in Peptides, Proteins, and Proteomes Using Visible Light. *J Am Chem Soc* **144**, 6227–6236 (2022).

20. Zanon, P. R. A. *et al.* Profiling the Proteome-Wide Selectivity of Diverse Electrophiles. *Chemrxiv* (2021).

21. Greulich, T. W., Daniliuc, C. G. & Studer, A. N -aminopyridinium salts as precursors for N-centered radicals - Direct amidation of arenes and heteroarenes. *Org Lett* **17**, 254–257 (2015).

22. Katritzky, A. R., Ranjan, Patel, C. & Shanta, M. 2-and 4-Pyridones by Oxidative Demethylation of 2-and 4-Methyl-Pyridinium Cations. *J. Chem. Soc., Perkin Trans **1***, 1888-1889 (1980).

23. Forman, H. J., Zhang, H. & Rinna, A. Glutathione: Overview of its protective roles, measurement, and biosynthesis. *Molecular Aspects of Medicine* **30**, 1–12 (2009).

24. Fava, A., Reichenbach, G. & Perón, U. Kinetics of the Thiol-Disulfide Exchange. II. Oxygen-Promoted Free-Radical Exchange between Aromatic Thiols and Disulfides. *J Am Chem Soc* **89,** 6697-6700 (1967).

25. Shin, D. *et al.* Regulation of Phosphoribosyl-Linked Serine Ubiquitination by Deubiquitinases DupA and DupB. *Mol Cell* **77**, 164-179 (2020).

Supporting information

General synthetic procedures

All reagents were used as received unless stated otherwise. Solvents used in synthesis were dried and stored over 4Å molecular sieves, except for MeOH and MeCN which were stored over 3Å molecular sieves. Triethylamine (TEA) and diisopropylethylamine (DIPEA) were stored over KOH pellets. TLC analysis was performed on Macherey-Nagel aluminium sheets (silica gel 60 F_{254}). TLC was used to visualize compounds by UV at wavelength 254 nm and by spraying with either cerium molybdate spray (25 g/L $(NH_4)_6Mo_7O_{24}$, 10 g/L $(NH_4)_4Ce(SO_4)_4{\cdot}H_2O$ in 10% H_2SO_4 water solution) or $KMnO_4$ spray (20 g/L $KMnO_4$ and 10 g/L K_2CO_3 in water) followed by charring at c.a. 250 °C. NMR spectra were recorded on a Bruker AV-300 NMR. Chemical shifts (δ) are given in ppm relative to tetramethyl silane. Coupling constants (*J*) are given in Hz. All given ^{13}C-APT spectra are proton decoupled.

LC-MS measurements and HPLC purifications

LC-MS measurements were conducted on a Waters ACQUITY UPLC H-class System equipped with a Waters ACQUITY Quaternary Solvent Manager (QSM), Waters ACQUITY UPLC Photodiode Array (PDA) eλ Detector (λ = 210-800 nm), Waters ACQUITY UPLC Protein BEH C18 column (1.7 µM, 2.1 x 50 mm) and LCT Premier Orthogonal acceleration Time of Flight Mass Spectrometer (m/z = 100-1600) in ES+ mode. Samples were run for 3min at 40 °C using 2 mobile phases: A: MQ + 0.1% formic acid, B: MeCN + 0.1% formic acid. Gradient: 0 - 95% B at a flow rate of 0.5 mL/min. Data processing was performed using Waters MassLynx Mass Spectrometry Software 4.1 (deconvolution with MaxEnt1 function).

HPLC purification was performed on a **A)** Shimadzu semi-preparative RP-HPLC system, equipped with a Waters C18-Xbridge 5 µm OBD (10 x 150 mm) column at a flowrate of 6.5 mL/min. using 2 mobile phases: A: MQ + 0.05% FA, B: MeCN + 0.05 % FA. Gradient: 10 -> 70% B. HPLC system **B**) Waters preparative RP-HPLC system, equipped with a Waters C18-Xbridge 5 µm OBD (30 x 150 mm) column at a flowrate of 37.5 mL/min using 3 mobile phases: A: MQ, B: CH_3CN and C: 1% TFA in MQ. Gradient: 20 -> 45% B, 5% C. High resolution mass spectra were recorded on a Waters XEVO-G2 XS Q-TOF mass spectrometer equipped with an electrospray ion source in positive mode (source voltage 3.0 kV, desolvation gas flow 900 L/hr, temperature 250 °C) with resolution R = 22000 (mass range m/z = 50-2000) and 200 pg/µL Leu-Enk (m/z = 556.2771) as a “lock mass”.

Chemical synthesis

α-1'-O-propargyl-5'-O-(2,4,6-trimethyl-1-pyridin-1-ium)-ribofuranoside (4)

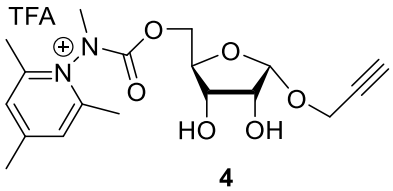

4

Pyridinium **4** was synthesized by adapting the procedure from Tower *et al*[18]., as follows:
α-1'-O-propargyl-2',3'-*O-iso*propylidene-ribofuranose **1** (20 mg, 0.087 mmol) and 1,1-carbonyldiimidizole (28.4 mg, 0.18 mmol, 2 eq.) were added to a flask and co-evaporated with toluene. Subsequently, the reactants were placed under argon atmosphere, dissolved in anhydrous MeCN (0.44 mL) and the reaction stirred for 4.5 h. Next, additional MeCN (0.2 mL) was added followed by methyl hydrazine (9.2 µL, 0.18 mmol, 2 eq.), and the reaction mixture was vigorously stirred at rt. After 1 hour, complete consumption of the starting material was detected by LC-MS. The reaction mixture was then concentrated *in vacuo* and co-evaporated with toluene to a afford the crude hydrazine **2**. The crude hydrazine and 2,4,6-trimethylpyrylium tetrafluoroborate (18.3 mg, 0.087 mmol, 1 eq.) were subsequently co-evaporated with toluene, placed under argon atmosphere and dissolved in EtOH (0.15 mL). After stirring the reaction mixture overnight, the red reaction mixture was concentrated *in vacuo*. Precipitation was attempted in DCM:EtOH (2:1 v/v ratio), but proved challenging at the performed reaction scale. The crude pyridinium **3** was then dissolved in a mixture of AcOH:H_2O (1 mL, 1:1 v/v) and stirred at 60 °C. After stirring for 2 days, LC-MS indicated complete deprotection of the i*so*propylidene group ($M + H^+ = 365$). The reaction mixture was diluted with toluene and concentrated *in vacuo*. Subsequent purification of the crude by preparative HPLC afforded pyridinium **4** (5.1 mg, 0.014 mmol, 16%) as a pale orange solid. **4** exists as a 1:1 mixture of rotamers at room temperature. ^{19}F NMR indicates **4** to be a TFA salt. ^{1}H NMR (300 MHz, MeOD) δ 7.90 (d, *J* = 8.7 Hz, 1H), 5.30 (d, *J* = 4.3 Hz, 0.5H), 5.09 (d, *J* = 4.2 Hz, 0.5H), 4.62 – 4.47 (m, 1H), 4.45 – 4.37 (m, 2H), 4.37 – 4.34 (m, 1H), 4.34 – 4.25 (m, 2H), 4.22 – 4.15 (m, 1H), 4.14 – 4.00 (m, 2H), 2.95 (td, *J* = 2.4, 0.8 Hz, 1H), 2.79 (dt, *J* = 7.5, 0.5 Hz, 3H), 2.76 (dd, *J* = 4.9, 0.6 Hz, 3H), 2.69 (dt, *J* = 4.5, 0.6 Hz, 3H). ^{13}C NMR (75 MHz, Methanol-d_4) δ 164.3, 159.0, 130.2, 101.9, 83.2, 82.8, 76.6, 73.1, 71.5, 69.2, 55.7, 38.3, 22.4, 19.2. ^{19}F NMR (282 MHz, MeOD) δ -76.98.

Rhodamine-Ub$_{76}$ (Arg42 → triazole linked 5'-O-pyridinium riboside) (5)

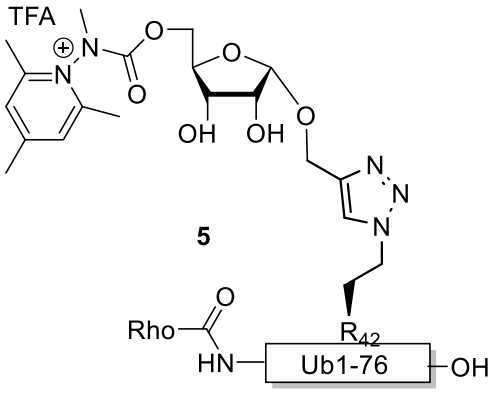

Pyridinium riboside **4** (15 µL, 0.15M in DMSO, 2.25 µmol, 4.0 eq) was added to a prepared solution of rhodamine ubiquitin bearing an Arg42 → azido homoalanine mutation (M + H$^+$ = 8873, 5 mg, 0.56 µmol, 1 eq) in DMSO (45 µL) and TRIS buffer (1.5 mL, 20 mM TRIS/150 mM NaCl, pH 7.6). To this was added 15 µL of freshly prepared click-mixture (1:1:1 v/v/v, $CuSO_4$ (100 mM in H_2O): Sodium Ascorbate (600 mM in H_2O): TBTA ligand (100 mM in MeCN). The reaction mixture was shaken at 37 °C for 30 min before the addition of another portion of freshly prepared click mixture (30 µL). After shaking for another 30 min, LC-MS verified complete conversion to the product (mass found: (M + H$^+$ = 9237). The conjugate was purified by RP-HPLC. Pure fractions were pooled and lyophilized obtaining ubiquitin-ribose conjugate **5** (3.1 mg, 0.033 µmol, 60%) as a red powder. HRMS: $[C_{414}H_{658}N_{111}O_{128}^+ + 7H]^{7+}$ found: 1320.6249, calculated: 1320.7814. $[C_{414}H_{658}N_{111}O_{128}^+ + 8H]^{8+}$ found: 11455.6383, calculated: 1155.8088. $[C_{414}H_{658}N_{111}O_{128}^+ + 9H]^{9+}$ found: 1027.2579, calculated: 1027.4967. $[C_{414}H_{658}N_{111}O_{128}^+ + 10H]^{10+}$ found: 924.5728, calculated: 924.8470. $[C_{414}H_{658}N_{111}O_{128}^+ + 11H]^{11+}$ found: 840.6064 calculated: 840.8609.

Photochemical cross-coupling of pyridinium probe 5 to Legionella effector enzymes, NRK-1 and DUBs

To a 96-wells plate containing buffer (20 mM TRIS, 150 mM NaCl, pH 7.6) the enzyme (Rho-Ub Arg42 to azido homoalanine, DupA, SdeA, NRK-1, UCHL-3 or USP-21, 10 µM), probe **5** (100 µM, 10 eq.) and optionally an additive (GSH, 1 mM or 300 µM) were added. The reactions were performed in a total volume of 50 µL and preincubated on ice for 15 min before irradiation using a 302 nm UV lamp (Analytikjena, UVP 3UV Lamp, 8 W), positioned on top of the 96-wells plate for 15 min, 30 min or 1 hour. The reaction mixture was then analyzed via LC/MS or SDS-PAGE. All experiments were performed with N=3 using the same protocol, and a single experiment is depicted as representative figure.

Photochemical cross-coupling of pyridinium probe 5 to DupA spiked into HEK293T lysate

To a 96-wells plate containing HEK293T cell lysate the enzyme (DupA, 2 µM), probe **5** (200 µM, 100 eq.) and GSH (300 µM) were added. The reactions were performed in a total volume of 25 µL and preincubated on ice for 15 min before irradiation using a 302 nm UV lamp (Analytikjena, UVP 3UV Lamp, 8 W), positioned on top of the 96-wells plate for 15 min. The reaction mixture was then analyzed directly via SDS-PAGE.

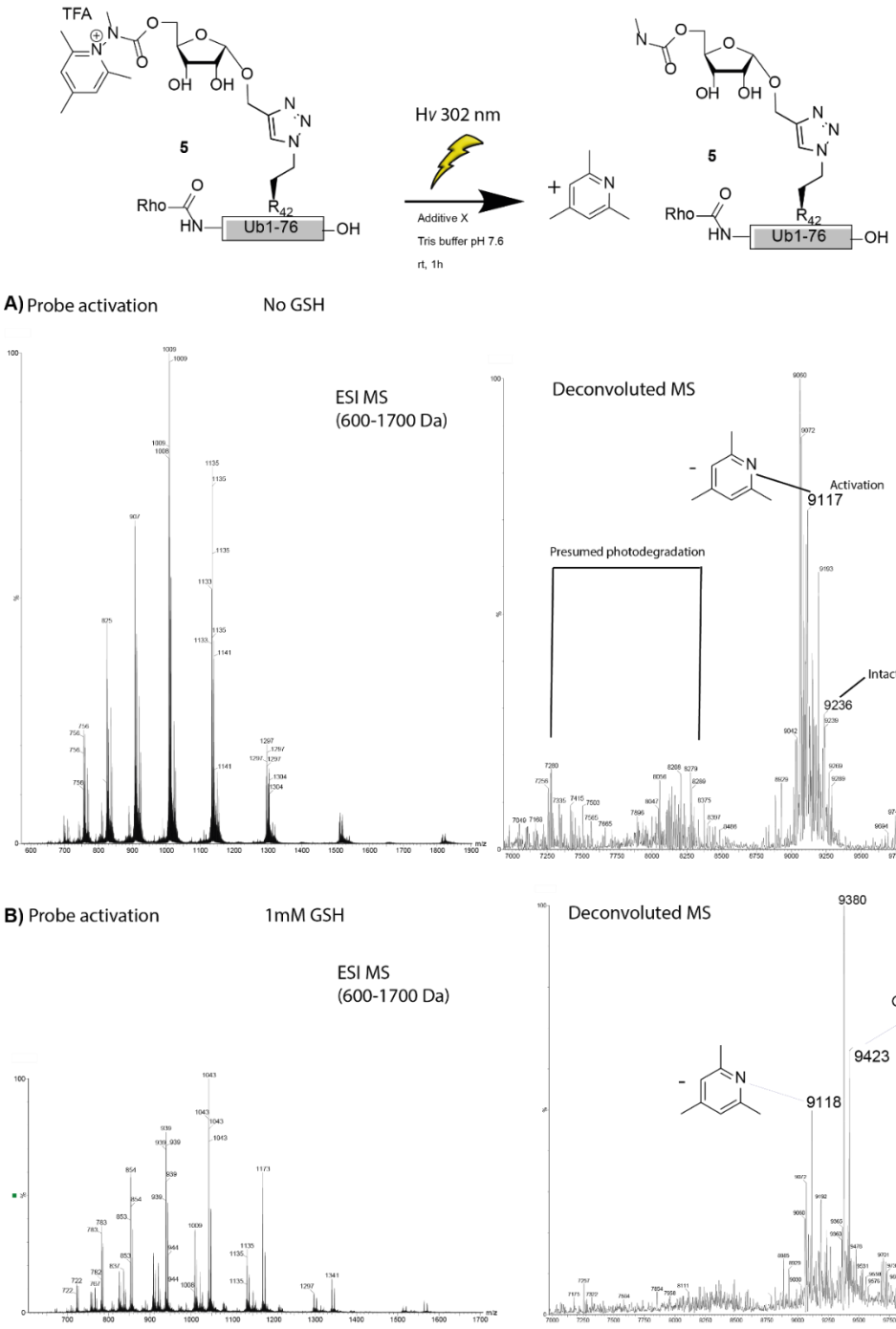

Supplementary Fig. 1. HRMS analysis of the activation of probe **5**. **A**) HRMS of the probe activation without GSH as additive. Probe activation is observed via loss of the pyridinium moiety ($M + H^+ = 9117$, $\Delta = 120$). Some residual starting material ($M + H^+ = 9236$) and presumed photodegradation products are as well detected, **B**) photoactivation of **5** in presence of GSH (1 mM). Probe activation ($M + H^+ = 9117$, $\Delta = 120$) as well as GSH addition ($M + H^+ = 9423$, $\Delta = 185$, concomitant loss of pyridinium moiety) are observed. The irradiation is performed for 1 hour at 302 nm.

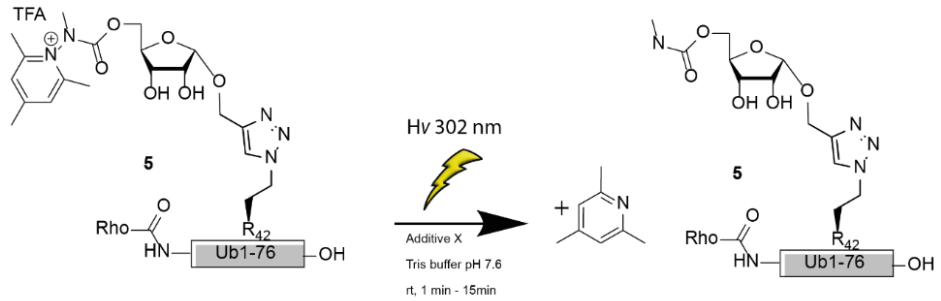

A) 1 min 300 µM GSH

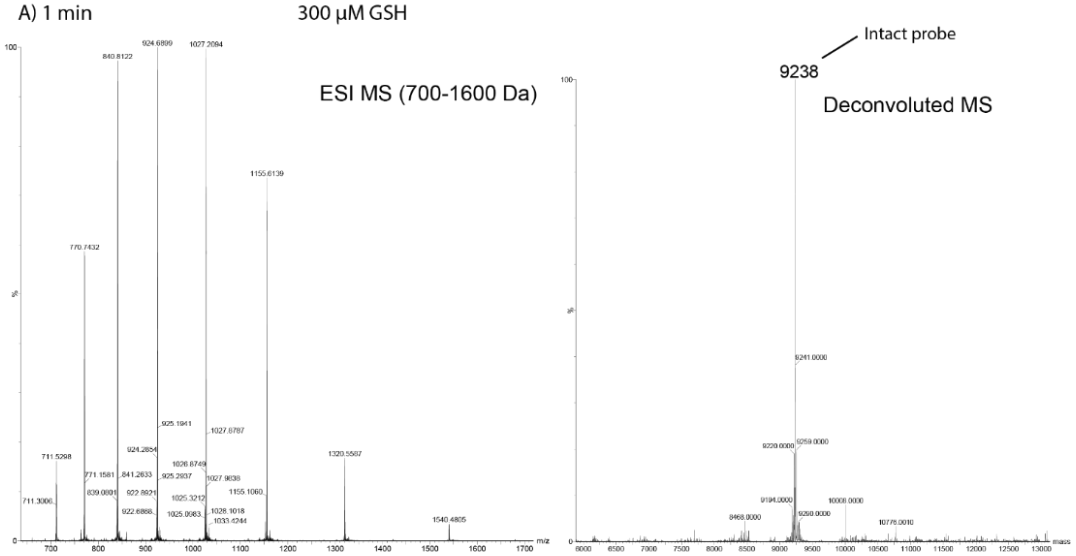

A) 15 min 300 µM GSH

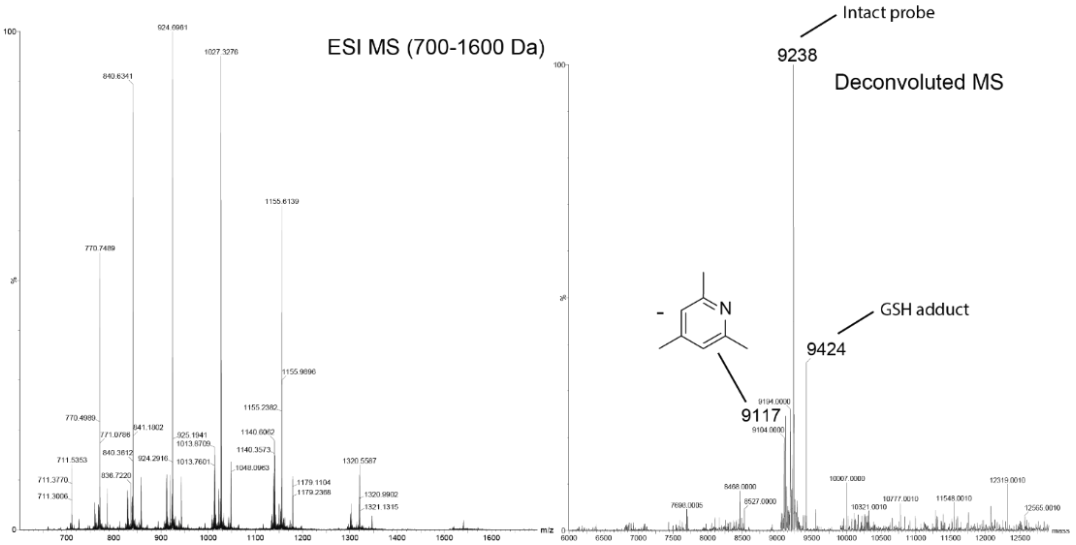

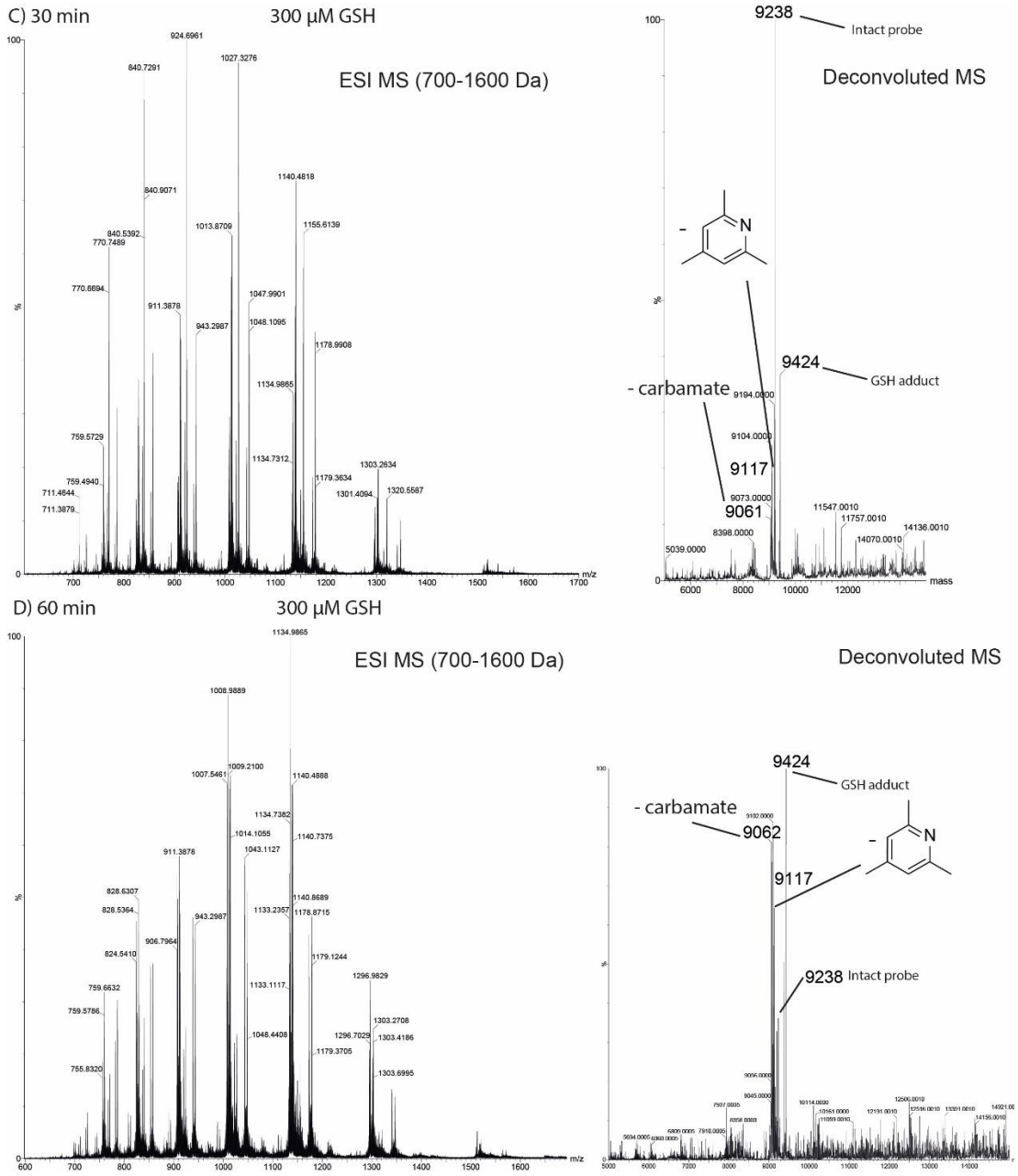

Supplementary Fig. 2. HRMS analysis of the activation of probe **5**. **A**) Probe **5** activation via 1 min of irradiation (302 nm) in the presence of GSH (300 µM) as additive. Predominantly intact probe ($M + H^+$) is detected, **B**) The photoactivation reaction analyzed after 15 min. Probe activation is observed via loss of the pyridinium moiety ($M + H^+ = 9117$, $\Delta = 120$) as well as GSH addition ($M + H^+ = 9423$, $\Delta = 185$, concomitant loss of pyridinium moiety) are observed, **C**) The photoactivation reaction analyzed after 30 min. Probe activation is observed via loss of the pyridinium moiety ($M + H^+ = 9117$, $\Delta = 120$) and concomitant loss of the carbamate moiety ($M + H^+ = 9062$). Residual starting material ($M + H^+ = 9236$) is as well detected, **D**) The photoactivation reaction analyzed after 60 min.

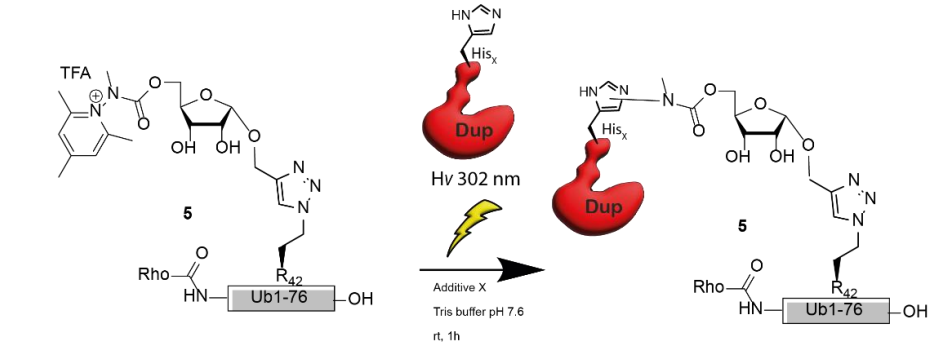

Supplementary Fig. 3. HRMS of the reaction between probe **5** and DupA irradiated for 1 hour at 302 nm. The reaction is monitored in the **A**) absence and, **B**) presence of GSH and analyzed by HRMS.

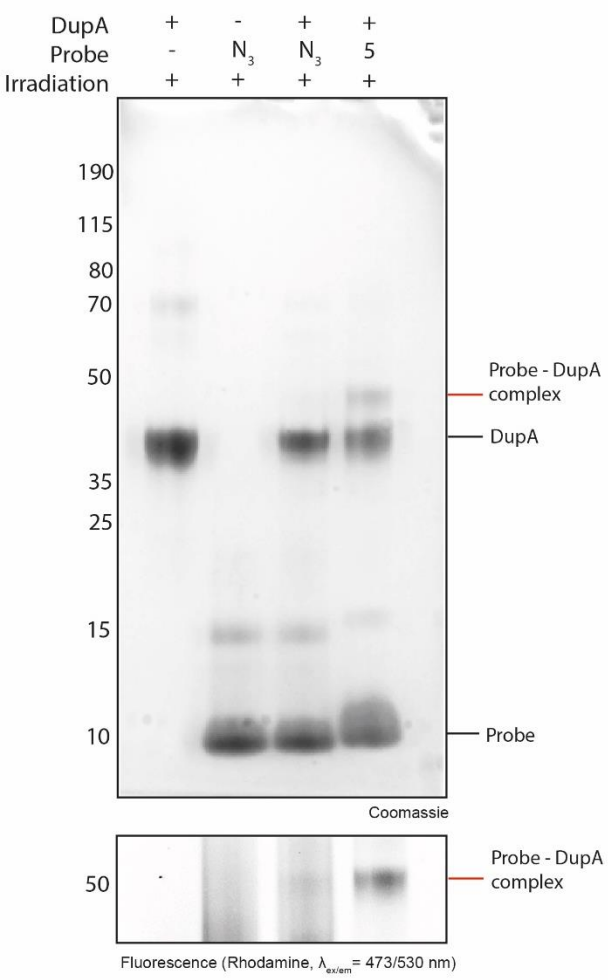

Supplementary Fig. 4. DupA does not crosslink to Rhodamine-(Arg42 to azido homoalanine) Ub_{76} (annotated as N_3) upon photoactivation, whereas it does with probe **5**. Irradiation is performed for 1 hour at 302 nm. Upper panel: Coomassie stained, bottom panel: Rhodamine fluorescence scan ($\lambda_{ex/em}$ = 473/530 nm).

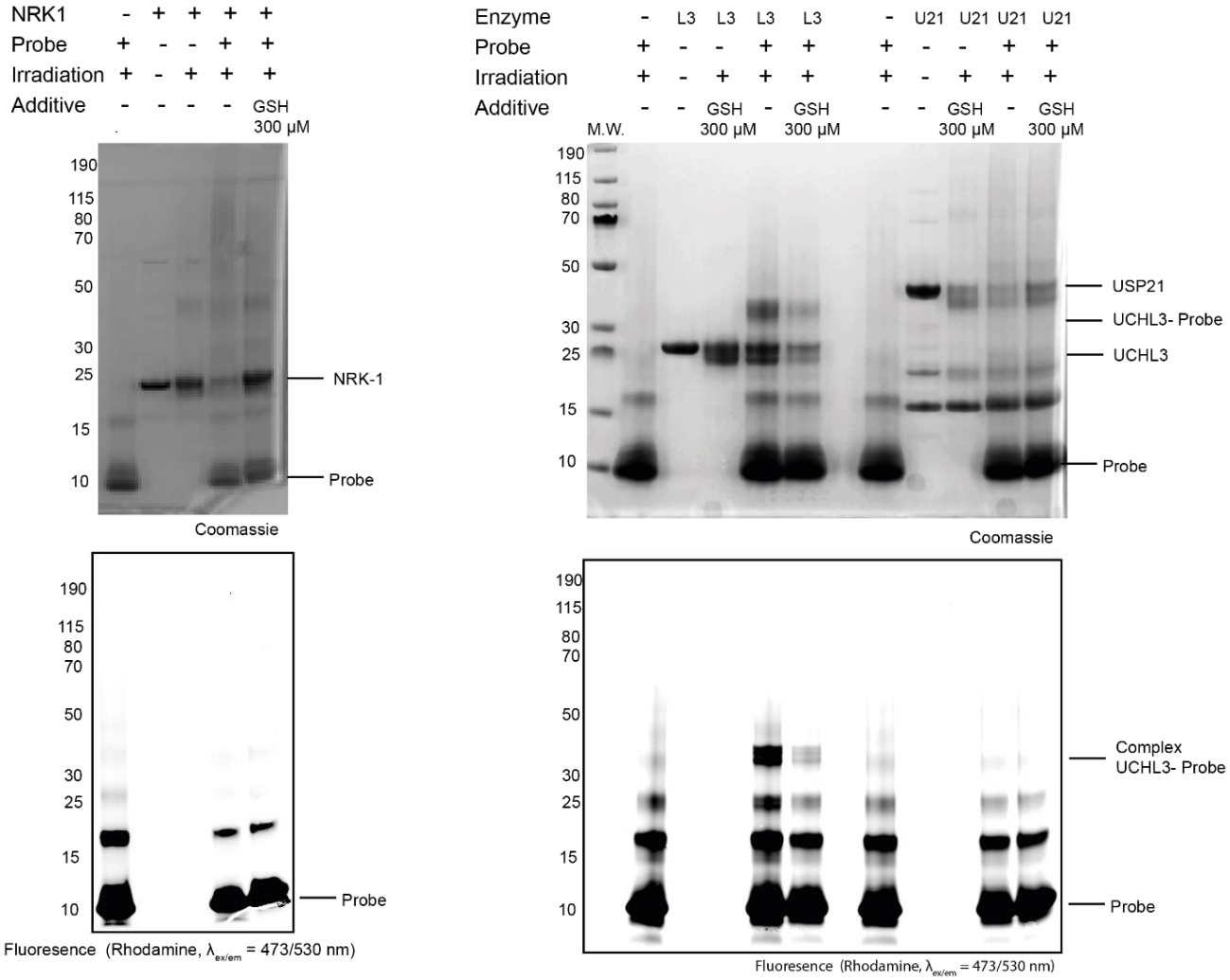

Supplementary Fig. 5. Ub pyridinium probe **5** binds UCH-L3 upon photoactivation. SDS-PAGE showing complex formation between probes **5** and UCH-L3 whereas no reaction for NRK-1 and USP21 is observed. Irradiation is performed for 1 hour at 302 nm. Upper panel: Coomassie stained, bottom panel: Rhodamine fluorescence scan ($\lambda_{ex/em}$ = 473/530 nm).

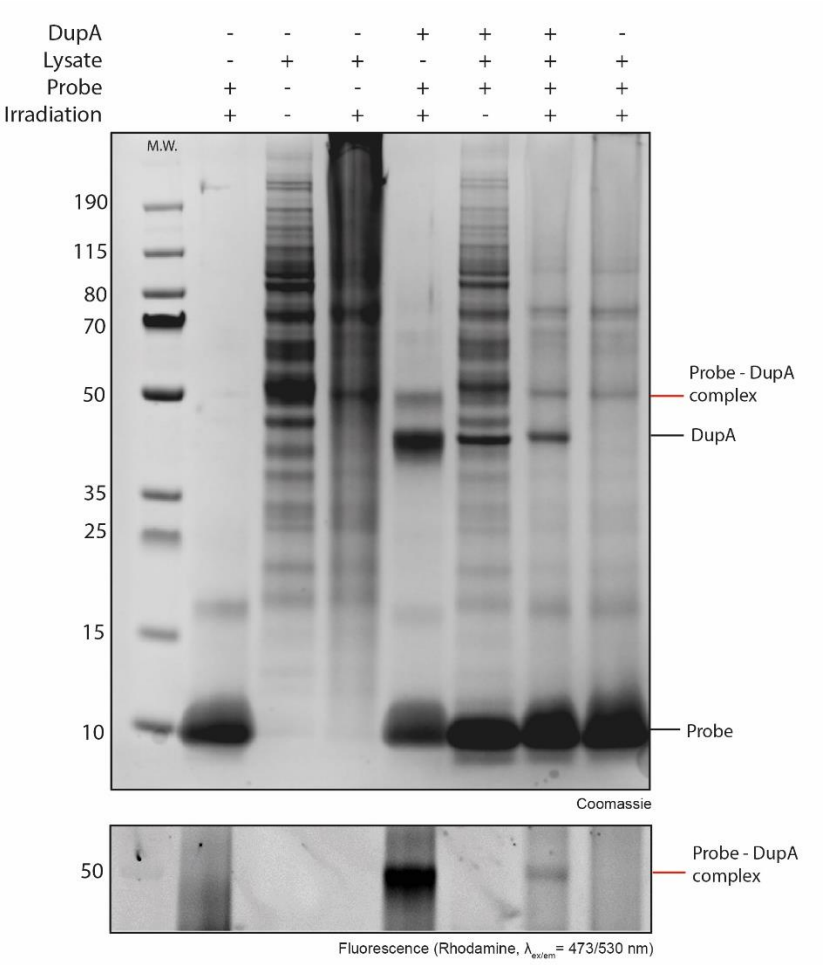

Supplementary Fig. 6. DupA (2 µM spiked in) labelling in HEK293T cell lysate using Probe **5** (200 µM). Irradiation is performed for 15 min at 302 nm. Upper panel: Coomassie stained, bottom panel: Rhodamine fluorescence scan ($\lambda_{ex/em}$ = 473/530 nm).

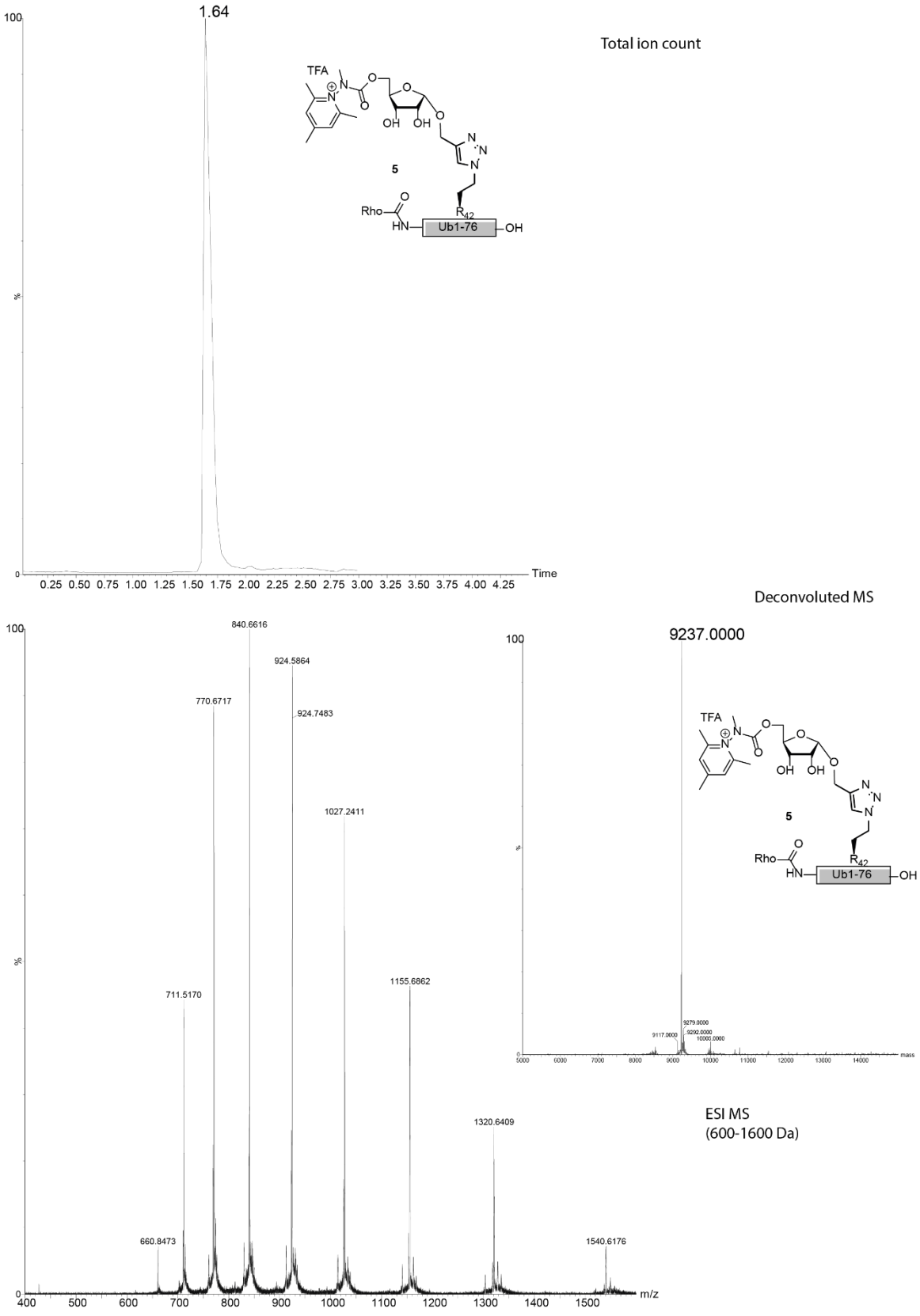

Supplementary Figure 7. HRMS spectra of Probe **5**.